12

Low Cost Multi-fiber Model Distributed Optical Fiber Sensor

Chuanong Wang
National Institute of Aerospace
Hampton, VA, USA

1. Introduction

1.1 Review on Techniques of Distributed Optical Fiber Sensors

Distributed optical fiber sensors are usable in many applications including stress monitoring of large structures such as buildings, bridges, dams, storage tanks, aircraft and also temperature profiling in electric power system, leakage detection in pipelines, etc. The researches on distributed optical fiber sensor are backward to 1970s (B. Lee, 2003; M. K. Barnoski & S. M. Jensen, 1976). Distributed optical fiber sensors are typically classed into intrinsic distributed optical fiber sensor and quasi-distributed optical fiber sensor. One of the most popular intrinsic distributed optical fiber sensors is optical time-domain reflectometry (OTDR) which is based on monitoring the Rayleigh backscattering along the fiber (M. Nakazawa, 1983). Based on the basic OTDR concept, various distributed sensing approaches were developed (A. J. Rogers, 1980; M. Zaboli & P. Bassi, 1983). OTDR has become a standard technique for testing optical fiber links and fault location in optical fiber communications. Furthermore, Raman OTDR, Brillouin OTDR and optical frequency-domain reflectometry (OFDR) (J. P. Dakin et al, 1985; M. Tateda, 1990; W. Eickhoff & R. Ulrich, 1981) are also developed and OTDR has found widespread applications in many fields (L. Thevenaz & M. Facchini, 1999). Concerning quasi-distributed optical fiber sensor, fiber bragg gratings (FBG) sensors are well developed and have been commercially manufactured and practically adopted on some bridges and dams (W. W Morey et al, 1990; W. L. Schulz et al, 1998).

1.2 Needs in Lower Cost Distributed Optical Fiber Sensors

Distributed optical fiber sensors offer many advantages over traditional sensor techniques especially in long distance distributed parameters measurement and electric critical environments. Moreover, optical fiber is a low cost medium which is essentially important for the sensors popular applications. Nowadays, fiber sensors can be found in long distance power line systems, in buildings, bridges, dams, vehicles and even aircrafts. However, most of distributed optical fiber sensor systems which are considered for a very long distance (generally over kilometers) are very costly. This is because the instruments for the light source and signal detections are very complex and costly. And in traditional distributed optical fiber sensor system, the signal detection and processing have been a

complex problem. For examples, Rayleigh OTDR has the disadvantage of a weak signal which has to be integrated over many pulses and leads to a long response time. Raman OTDR is more serious because Raman scattering coefficient is about three orders of magnitude weaker than that of the Rayleigh (J. P. Dakin et al, 1985). Although several improving approaches are proposed to enhance the capability of detecting the weak backscattering signal (J. K. A. Everard, 1987), the fundamental limitation of conventional OTDR brings many difficulties on signal detection where great bandwidth leads to low signal noise ratio. Brillouin OTDR and OFDR not only have very weak scattering signals but also need coherent detection which makes the total system more sophisticated. FBG sensor, which integrates many fiber Bragg gratings in a single fiber, is based on wavelength division multiplexing technique and needs complex techniques for manufacturing. Therefore, all the current distributed optical fiber sensing techniques are based on complex signal detection and processing techniques which leads to sophisticated instruments such as reflectometry and interferometer. The entire sensing systems are complex and costly. In the applications of distributed optical fiber sensors, the cost of sensor systems limits the application of distributed optical fiber sensor to the objectives only having great importance. Actually, optical fiber sensors are desired in most structures which need distributed parameter measurement. There are wide needs of distributed optical fiber sensors in middle length (several meters to several hundred meters) with simpler system and lower cost.

1.3 Multi-fiber Model Sensor Concept

In recent years, a new technique was developed motivated by the low cost applications in middle distance range (C. Wang & K. Shida, 2006, 2007). The concept of new technique is to use light coupling between multi-fiber (generally two fibers) and the attenuation of light over fibers for distributed sensing. Basically, the sensor uses transmission light active fiber for localized deformation measurement and the coupling light from active fiber to passive fiber for position information. The output of sensor can be detected by photodiodes with a simple preamp circuit. The principle of the new sensor eliminates all the critical requirements on light source and signal detection as in conventional OTDR and FBG sensors. Therefore, the light source and signal detection circuit are very simple and low cost. Although more fibers are used, the total sensor system cost is greatly reduced because the cost of light source and signal detection instrument are greatly reduced.

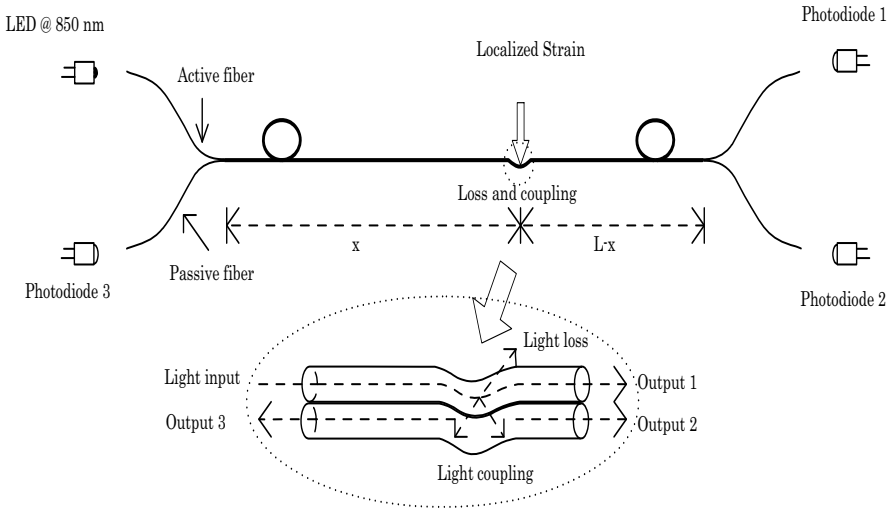

Fig. 1. Structure and principle of the multi-fiber model sensor.

The sensor here is different with evanescent wave coupling based sensors where the evanescent wave power in the cladding of single model optical fiber is quite weak. We use multi-model fibers for both active fiber and passive fiber. This multi-fiber model sensor is a new attempt for distributed optical fiber sensor except the techniques reviewed above. The idea is confirmed by the prototype sensors. The theoretical model and analysis on maximum length and spatial resolution are also studied.

2. Principle, Theory, Design of Intrinsic Distributed Multi-fiber Model Sensor

2.1 Structure and Principle of Sensor

As illustrated in Fig.1, the sensor is composed of two fibers. The first fiber is defined as the active fiber with light propagating within it. The second fiber is defined as the passive fiber which has no active light inside in common state and is designed to receive coupling light from the active fiber passively. The transmission rate of the active fiber is sensitive to the strain applied on it. By analyzing the output of active fiber, strain value can be measured. The response of the active fiber to strain has no dependency on the strain position. When localized strain is applied on the two fibers, light couples from the active fiber to the passive fiber at the strain applied point. The coupled light propagates along the passive fiber in the direction of both forward and backward. The outputs at the two ends of the passive fiber (output 2 and output 3) are used for strain position determination. Distributed sensing is based on the passive fiber attenuation. Fiber attenuation may be caused by absorbency, scattering, disfigurement of structure, bending and so on. The transmission characteristics of a fiber are usually given in terms of attenuation for a given wavelength (or range) and over a given length. The elementary experimental experience gives the relation of transmission rate and attenuation coefficient as follow:

$$T_r = \frac{P_{out}}{P_{in}} = 10^{-\frac{L\cdot\alpha}{10}} \tag{1}$$

where, α is attenuation coefficient, L is the length of fiber, P_{in} is the input light intensity, P_{out} is the output light intensity, T_r is the transmission rate. Obviously, the transmission rate of fiber has dependency on attenuation coefficient and length of fiber. When attenuation coefficient is fixed, the transmission rate is only related to the length of fiber. Therefore, if light is limited into a fiber at a certain point of the medium part, the output light intensities at two ends have dependency on the light incident position. Concerning the proposed sensor in this paper, different strain positions result in different outputs at the two ends of the passive fiber. By analyzing the output light intensities at the two ends of passive fiber, the position of strain can be determined. Attenuation coefficient of common fiber is generally smaller than 10 dB/km in the communication systems and has the theoretical limit of 0.2 dB/ km. In our study, the passive fiber is designed to have condign attenuation coefficient which is greater than common fiber.

2.2 Light Source and Signal Detection Circuit

We use a LED (Hamamatsu Co. L7560) as the light source of the active fiber which has a peak wavelength at 850 nm. The typical coupled light power of 30 μW is taken as the effective light emitting power of LED for analysis. Three photodiodes (Centronic Co. OSD1-5T) are used as the light detectors which has peak responsivity of 0.45 A/W at wavelength of 850 nm. The noise equivalent power (NEP) of the photodiodes is 25 fW. AD549 is used for the preamp of photodiodes which has a low offset drift by temperature of 20 μV/°C. The preamp electric circuit is shown in Fig. 2. The principle of the preamp electric circuit gives the expression of output voltage as follow:

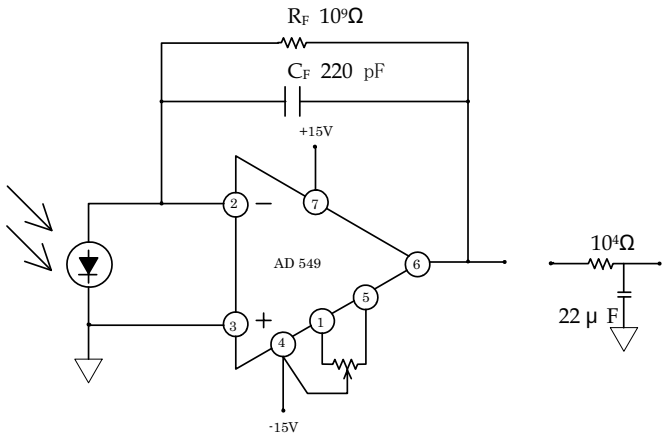

Fig. 2. Electric circuit for photodiode signal amplifying.

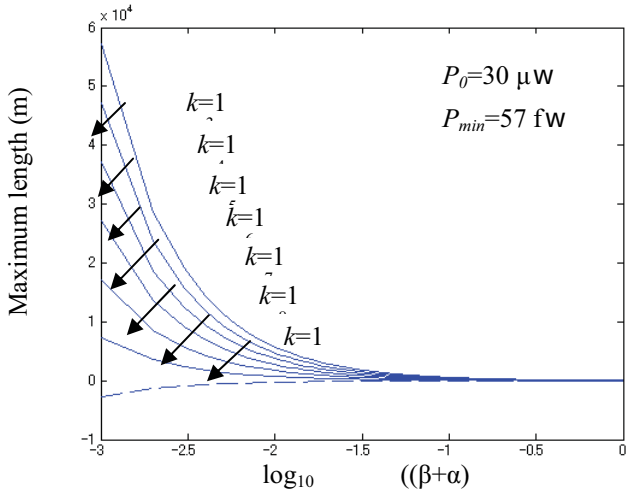

Fig. 3. Length limit of multi-fiber model sensor with different coupling coefficients.

$$V_{out} = P \times R \times \frac{R_F}{1 + j \cdot (f / f_p)} \tag{2}$$

where P is the light power incident on the photodiode surface in Watts and R is the photodiode peak responsivity of 0.45 A/W, f is signal frequency and f_p is the 3 dB cutoff frequency equals to:

$$f_p = \frac{1}{2\pi \cdot R_F \cdot C_F} \tag{3}$$

C_F sets the signal bandwidth to 0.7 Hz with R_F and also limits the peak in noise gain that multiplies the op amp input voltage noise contribution. A single pole filter at the amplifier output limits the op amp output voltage noise bandwidth to 0.7 Hz which improves the preamplifier's signal to noise ratio by a factor of three. Noise limits the signal resolution obtainable by the preamp. The photodiode preamp circuit in Fig. 2 can detect a signal current of 26 fA rms. Since the photodiode has responsivity of 0.45 A/W, the minimum detectable light power is 57 fW which is about double of the photodiodes noise equivalent power (NEP) 25 fW. The dynamic range of the preamp can be adjusted in practical applications.

2.3 Theory and Analysis on Limit Parameters

The maximum length of double-fiber distributed optical fiber sensor is restricted by the output light power at the passive fiber ends and the minimum detectable light power by photodiode preamp. From the principle of sensor, the emitting light intensities at the tow ends of passive fiber can be expressed as follow:

$$P_f = P_0 \cdot k_e \cdot 10^{-\frac{\alpha \cdot x}{10}} \cdot k_s \cdot k_f \cdot 10^{-\frac{\beta(L-x)}{10}} \tag{4}$$

$$P_b = P_0 \cdot k_e \cdot 10^{-\frac{\alpha \cdot x}{10}} \cdot k_s \cdot k_b \cdot 10^{-\frac{\beta \cdot x}{10}} \tag{5}$$

where

P_f emitting light intensity at forward end of passive fiber;
P_b emitting light intensity at backward end of passive fiber;
P_0 effective emitting light intensity of LED;
k_e input end coupling coefficient;
a attenuation coefficient of active fiber;
x position of localized strain;
k_s coupling coefficient from active fiber to passive fiber by strain;
k_f fraction of light propagating forward within the passive fiber;
k_b fraction of light propagating backward within the passive fiber;
β attenuation coefficient of passive fiber.

Since the double ended outputs of passive fiber are used for position sensing, the length limiting conditions are that $P_f > P_{min}$ at position of $x = 0$ and $P_b > P_{min}$ at position of $x = L$. Educing (4) and (5) by these limiting conditions, we can get the length limiting equations as follow:

$$L < \frac{10}{\beta} \log_{10}\left(\frac{P_0 \cdot k_e \cdot k_s \cdot k_f}{P_{\min}}\right) \tag{6}$$

$$L < \frac{10}{\beta + \alpha} \log_{10}\left(\frac{P_0 \cdot k_e \cdot k_s \cdot k_b}{P_{\min}}\right) \tag{7}$$

where, P_{min} is the minimum detectable light intensity by the preamp. The attenuation of active fiber is expected to be minimized while that of the passive fiber is quite greater. The attenuation is mainly caused by the passive fiber. Moreover because of the similarity of the output expressions at the two ends of the passive fiber, we can use (7) for the analysis of outputs at both ends.

The theoretical length limit to attenuation coefficient is shown in Fig. 3 where we define $k=k_e \cdot k_s \cdot k_f$ or $k=k_e \cdot k_s \cdot k_b$ as the total effective coupling coefficient. From the calculation results, we can see that lower attenuation coefficient and higher total effective coupling coefficient conduce to greater length limit. The length limit greatly depends on the total effective coupling coefficient k. In practical experiments, to nondestructive strain, k is at the factor of 10^{-7} -10^{-3} and for destructive strain, k is at the factor of 10^{-3}-10^{-2}. By designing appropriate attenuation coefficient of passive fiber, the fibers length can reach the level of kilometers which is meaningful for many applications in structure strain monitoring such as bridges and dams.

Because of the exponential attenuation of light propagating in fiber, the spatial resolution of the proposed sensor is non-uniform along the length of fiber. The minimum spatial resolution Δx by single end output is restricted by the conditions expressed as follow respectively:

$$P_f(x + \Delta x) - P_f(x) > P_{\min} \tag{8}$$

$$P_b(x) - P_b(x + \Delta x) > P_{\min} \tag{9}$$

where $P_f(x)$ and $P_b(x)$ are output light power at forward and backward end respectively corresponding to coupling position of x. From the above two equations, we can get the spatial resolution distribution along the fiber as follow:

$$\Delta x_f = \frac{10}{\beta - \alpha} \cdot \log_{10}[1 + \frac{P_{\min} \cdot 10^{\beta L} \cdot 10^{(\alpha-\beta)x}}{P_0 \cdot k_e \cdot k_s \cdot k_f}] \tag{10}$$

$$\Delta x_b = \frac{10}{\beta + \alpha} \cdot \log_{10}[1 - \frac{P_{\min} \cdot 10^{\beta L} \cdot 10^{(\alpha-\beta)x}}{P_0 \cdot k_e \cdot k_s \cdot k_b}]^{-1} \tag{11}$$

where Δx_f and Δx_b are the spatial resolutions determined by the single end output of forward and backward respectively. The spatial resolution distributions are greatly influenced by the parameters of k_f and k_b. In Fig. 4, we show the single end determined spatial resolution distributions under three groups of k_f and k_b. The length is 1000 m and (k_f , k_b) equals to (0.9, 0.1), (0.7, 0.3) and (0.5, 0.5) respectively. From (4) and (5), we can see that the outputs light intensities at both ends of the passive fiber have dependence on k_s, which is influenced by strain value. Therefore, dividing (4) by (5), we can get k_s independent equation as follow:

$$x = \frac{1}{2}[L + \frac{10}{\beta}\log_{10}(\frac{P_f}{P_b} \cdot \frac{k_b}{k_f})] \tag{12}$$

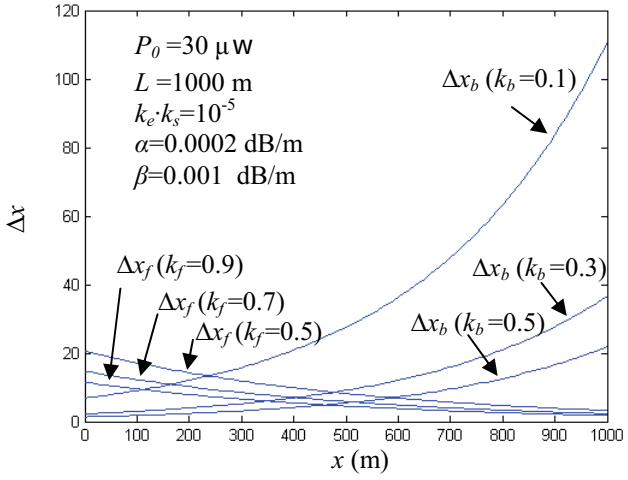

Fig. 4. Spatial resolution distribution by single end output.

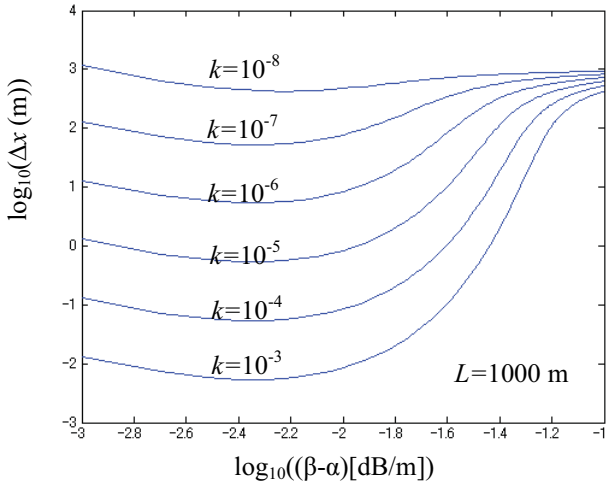

Fig. 5. Spatial resolution dependence on attenuation coefficient of passive fiber when L =1000 m.

In (12), the strain position in theory has no dependency on k_s, the coupling coefficient between the two fibers. Actually, the strain value has influence on position sensitivity. Smaller strain value leads to less sensitivity to position and the position estimation is restricted by the detectable conditions. Since P_f and P_b have different individual sensitivity to position, the total spatial resolution is determined by the more sensitive one as follow:

$$\Delta x = \min\left\{\Delta x_f, \Delta x_b\right\} \tag{13}$$

From the spatial resolution distribution illustrated in Fig. 4, we can see that the total spatial resolution Δx has a maximum value at the point where Δx_f is equal to Δx_b. To nondestructive strain, the coupling light propagating forward within the passive fiber is much more than that of backward, the parameter k_f is quite greater than k_b. The total spatial resolution mainly depends on the forward end output. For convenience of analysis, we use the restricting condition expressed in (10) at point of x=0 for total spatial resolution analysis. This is a conservative condition and in theory the spatial resolution can be better. The total spatial resolution to attenuation coefficient is shown in Fig. 5 where we suppose the length is 1000 m. From the calculational results, we can know that, the attenuation coefficient has an optimization area for the best spatial resolution on a given length. Spatial resolution greatly depends on the total effective coupling coefficient k which is also illustrated in Fig. 5. From the figure, we can see that, if the total effective coupling coefficient k is at the level of 10^{-7}, it will be meaningless for the spatial resolution of hundred meters. When k changes from 10^{-6} to 10^{-5}, the spatial resolution can be promoted from tens of meters to the level of meter with appropriate attenuation coefficient. When k changes from 10^{-5} to 10^{-3}, the spatial resolution is furthermore promoted to centimeter level. In spite of other factors, higher coupling coefficient is propitious to the promotion of spatial resolution.

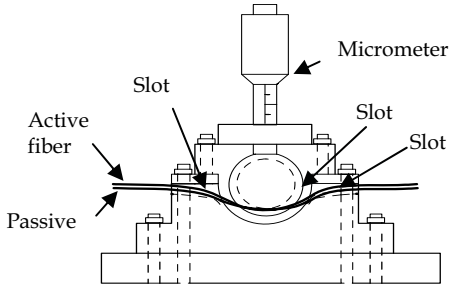

Fig. 6. Experimental micrometer controlled mechanism for strain.

However, in practical experiments, the high coupling coefficient is at cost of great destructive strain which leads to an unsteady relationship between k_f and k_b. As expressed in (12), the ratio of k_b to k_f has direct influence on the position value estimation. As a matter of fact, k_b and k_f are influence by strain value. To the same strain, the ratio of k_b to k_f is constant. To value changeable strain, k_f and k_b should be determined before the position estimation. It is more difficult for destructive strain with a high coupling coefficient than that of the nondestructive strain. Anyway, even in the area of nondestructive strain, spatial resolution can reach a level which is meaningful to many applications. All the above analysis is restricted by the given LED emitting light power 30 μW which has much space to be promoted. Greater light emitting power of light source contributes to promotion of length and spatial resolution and also decreases the influence of coupling coefficient. Optimized designing of the double-fiber model sensor is a tradeoff between the length and spatial resolution for attenuation coefficient of the passive fiber.

2.4 Experiments on Prototype Sensor

The prototype sensor is developed with a length of 4 meters. Two multi-model fibers are used for both the active and passive fiber with the attenuation coefficient of 0.007 dB/m and 3.5 dB/m respectively. The attenuation is mainly caused by the passive fiber and the attenuation caused by the active fiber can be ignored. A fiber light source aimed LED is used for light emitting. Three high sensitive photodiodes are used for light detection. AD549 is used for the preamp electric circuit and the preamp is designed to have a narrow bandwidth of 0.7 Hz together with a low-pass filter in order to promote the signal to noise ratio. A digital multimeter (KEITHLEY 2000) is used for voltage signal measurement and the data is automatically recorded by a computer. We use a micrometer controlled mechanism to apply strain on the two fibers as illustrated in Fig. 6. The mechanism uses a cylinder in radius of 1 cm to apply strain on fibers. Both of the cylinder and the base parts are machined with slots to hold the fibers. The two fibers keep vertical through the whole process of experiment. The applied strain on fibers can be precisely controlled to both nondestructive and destructive strain. Experiments are made in laboratory room with temperature roughly controlled. The transition process of LED and electric circuit are well considered by making experiments after waiting a period of time. The room light is well shielded to avoid noise caused by disorder light.

Light coupling coefficient includes the input end coupling coefficient k_e and the strain coupling coefficient k_s. The LED L7560 has a small lens integrated at the front part which is specially designed for light emitting into fiber. The input end coupling coefficient k_e is 0.462 under the conditions of our experiments. The light coupling coefficient between the two fibers k_s is an important parameter to the proposed sensor. The output light intensities of the passive fiber greatly depend on the light coupling coefficient, and consequently, the maximum length and the spatial resolution. The coupling coefficient is dependent on applied strain value. The experimental results of light coupling coefficient are shown in Fig. 7 where the k_{ef} and k_{eb} are the total effective coupling coefficient in forward and backward direction which are equal to $k_e \cdot k_s \cdot k_f$ and $k_e \cdot k_s \cdot k_b$ respectively. According to the deformation value of fibers, the applied strain can be divided into the nondestructive strain and the destructive train. From the experimental results, we can see that, k changes from 10^{-5} to 10^{-3} in nondestructive strain area and changes from 10^{-3} to 10^{-2} in the destructive strain area. The theoretical maximum length can be up to the level of 10 km and the spatial resolution can be under the level of centimeter in spite of other factors.

Since (12) is independent from k_s, the effectiveness of position estimation will not be influenced by changes of light coupling coefficient k_s as long as the output light intensities are under the restricting conditions of length limit and spatial resolution. The ratio of backward propagating light and forward propagating light directly influence the position estimation as illustrated in (12). If the same strain is applied on different position of sensor, the ratio of k_b to k_f has the same value. Consequently, (12) works well for stain position estimation. However, if different strain values are applied, the ratio of k_b and k_f must be determined before strain position estimation.

As illustrated in Fig. 7, the effective coupling coefficient has different dependence on the strain value in the two areas of nondestructive and destructive strain. In the nondestructive strain area, both of the k_{ef} and k_{eb} have exponential form dependence

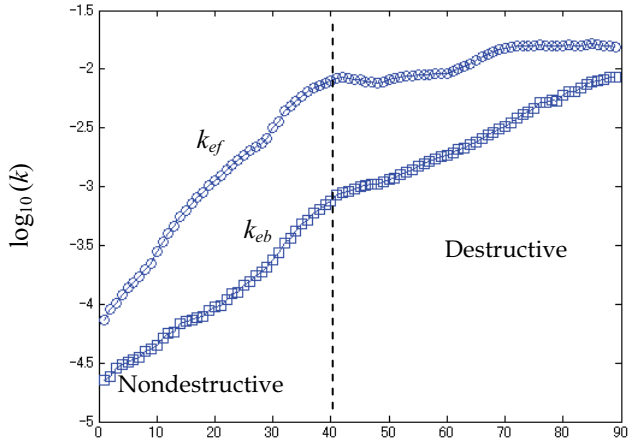

Fig. 7. Experimental results of light coupling coefficients.

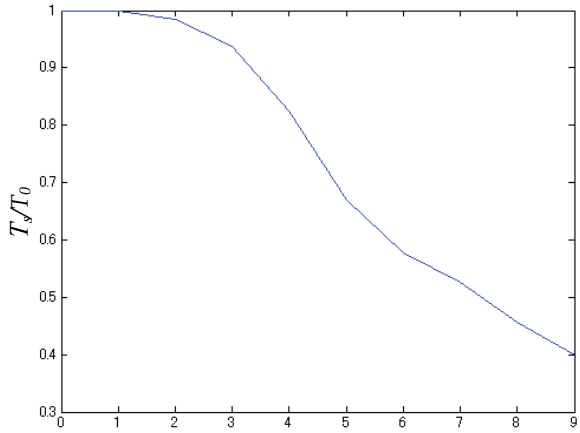

Fig. 8. Response of the active fiber transmission rate to strain value.

on strain value which can experientially be modeled. In the destructive strain area, the forward effective coupling coefficient k_{ef} shows unstable dependence on strain value which brings difficulties for value estimation. Therefore, under current conditions, the proposed sensor is used in the area of nondestructive strain. Concerning the applications such as civil structure strain monitoring, it is of the same importance to detect the exceptional strain in the early stage with warning the accidental destructive strain.

The active fiber is used for strain value sensing. The response of active fiber transmission rate to the strain value is shown in Fig. 8, where T_s is the transmission rate of the active fiber with strain, T_0 is the original transmission rate. Although the active fiber used in our study is not specifically designed for pressure sensing, the active fiber has a sensitive response to the applied strain. Using the output of the active fiber, the strain value can be determined. In the area of nondestructive strain, the coupling coefficient can be consequently estimated. As a matter of fact, the transmission rate of the active fiber is not only dependent on the applied strain but also other factors, for example, ambient temperature and fiber eroding. The output of the active fiber includes all the perturbation on the fiber. However, strain can be indicated from other perturbations by the outputs of passive fiber. Moreover, the influence by ambient temperature is possible compensated by electrical circuit. The influence by localized high temperature area, for example, caused by fire, is another problems involved for further study.

In order to confirm the distributed sensing of the proposed sensor, we apply the localized nondestructive strain on the developed prototype sensor at different positions. In Fig. 9, we show the comparison of the practical experiment results and the theoretical curves predicted by (12), where the ratio of P_f to P_b is used for strain position estimation. From Fig. 9, we can see that, the experimental results are well coincident to the curves predicted by theoretical equation. The ratios of k_b to k_f under three strain values are experimentally tested to be 0.75, 0.57 and 0.43 respectively.

Concerning the strain position value reconstruction, we proposed the (12) which is confirmed by experimental results. Equation (12) eliminates the influence of k_s under the detectable conditions. But it is still influenced by the ratio of k_b to k_f. The

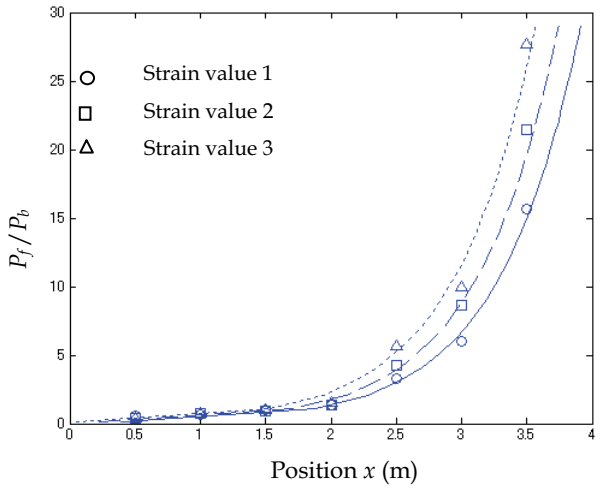

Fig. 9. Response of the passive fiber to distributed strain.

errors of position sensing mainly come from the estimation results of the ratio of k_b to k_f which can be modeled only in area of nondestructive strain. Therefore, the coupling model between the two fibers is of great importance to the proposed sensor. More precise model is achieved, the sensor provides better performance. When the ratio of k_b to k_f is fixed or experimentally measurable, the proposed sensor has great potential in spatial resolution and length. As another way, if the absolute value of k_{ef} can be determined, the strain position can be reconstructed by (4) individually. In Fig. 9, if the position goes on increasing, the

P_f / P_b will get sharp increase and it is not good for position sensing. However, the attenuation coefficient of passive fiber 3.5 dB/m is designed for 4 m length. To longer length, the attenuation coefficient of passive fiber has to be redesigned. As a matter of fact, optimizing and design of sensor need many strategies. To any given length applications, the response of passive fiber to strain position is expected to have similar form as shown in Fig. 9 with different x units.

As a result, the prototype sensor is effective to sense the distributed strain by the outputs of the passive fiber. The effectiveness of the proposed sensor is conformed. Moreover, both of the theoretical analysis and practical experiments are restricted by the given LED light emitting power 30 μm in this period of study. By using light emitting power promoted light source, the sensor can achieve better performance.

3. Quasi-Distributed Multi-fiber Model Sensor

3.1 Principle and Configuration of Quasi-Distributed Sensor

In intrinsic distributed multi-fiber sensor, the coupling coefficients ratio in forward and backward direction is dependent on fibers' deformation form which is uncertain in practical applications. And also, the backward coupling coefficient is quite smaller than forward coupling coefficient which limits the position sensing. Quasi-distributed sensor uses the special designed mechanism as the sensing element and has steady deformation form controlled by the mechanism. The light direction influence on coupling coefficient is also removed by using light sources at both ends of the active fiber so that the sensor has the symmetrical coupling coefficients in the two directions of forward and backward along the fiber. As illustrated in Fig.10, the sensor is composed of two multimode fibers with discrete sensing elements arranged along them. The first fiber is the active fiber with active light propagating within it. The second fiber is the passive fiber which has no active light inside in common state and is designed to receive coupling light from the active fiber. Strain sensing is performed by the sensing elements which are discretely arranged along the fibers with given distance interval. When localized strain is applied on certain sensing element, the two fibers are forced to macro bending by the sensing element. The jacket layers of the two fibers are divested in the sensing element parts. Therefore, the macro bending makes light lose from the active fiber and partly couple into the passive fiber. The coupled light propagates along the passive fiber mainly in forward direction. Light sources are used at both ends of the active fiber. Using this method, the light direction influence on coupling coefficient is removed. The outputs at two ends of the passive fibers will not be influenced by light propagating direction in the active fiber. The sensing elements are machined to have symmetrical inner shape (along the fibers' center axis) and fixed bending radius. This is motivated by the making symmetrical deformation of fibers along theirs center axis. Consequently, the coupling coefficients in the two opposite directions can be equal. The two fibers have jacket layers to protect fibers and prevent light coupling in other places outside the sensing elements. Therefore, the light coupling between the two fibers is limited in the sensing elements and with fixed deformation form. Using this method, the deformation form influence on the coupling coefficient is removed.

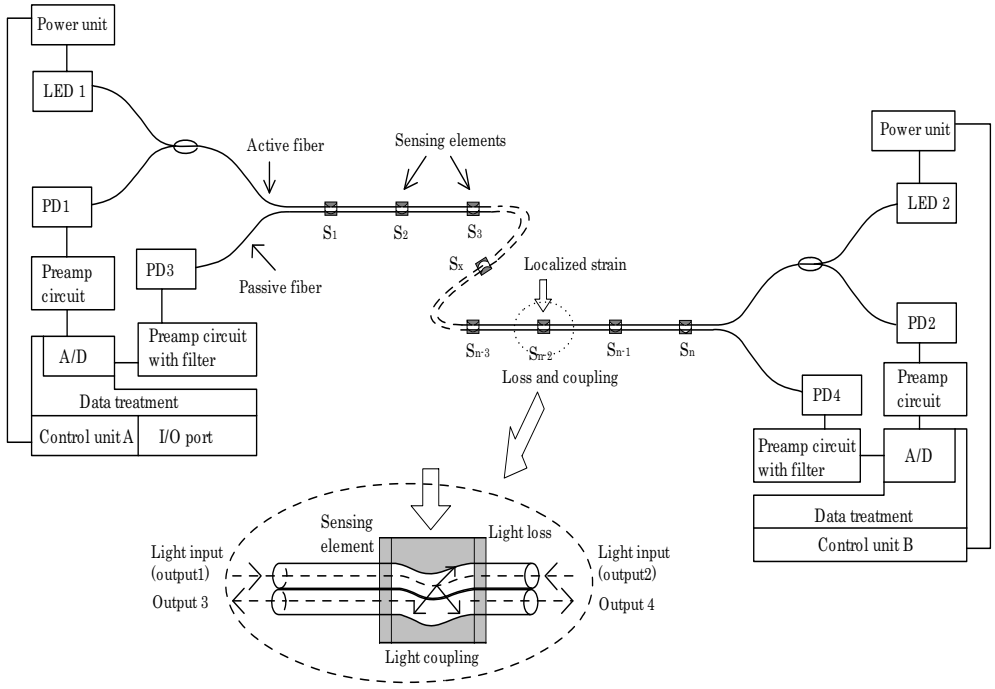

Fig. 10 Principle and configuration of the quasi-distributed sensor system

The sensor configuration is shown in Fig. 10. Two light-emitting-diodes (LED1 and LED2) are used as the light sources and two photo-diodes (PD1 and PD2) are used as the light detectors at two ends of the active fiber. The light-emitting-diode and photo-diode are connected to the active fiber by 3-dB coupler. Another two photo-diodes (PD3 and PD4) are used at the two ends of the passive fiber as the light signal detectors of the passive fiber. The circuit modules used in the sensor system are also illustrated in Fig. 10 including preamp circuits, filters, A/D converters, control units and power units.

As shown in Fig. 10, the driving circuits of the sensor system are divided into two parts which have different physical locations (at the two ends of the fibers). The active fiber (together with PD1 and PD2) is used not only for strain sensing and but also for handshaking commands and data communication between the two parts of the driving circuits. The working flow chart of sensor system is shown in Fig. 11. As the non-working state of the sensor system, the signal detection channel with PD2 keeps "listening" state to the active fiber output while other parts of the sensor system can be shut off in this state. Once measurement is started by manual operation or remote controlling signal, the control unit A firstly sends the "Start" command codes into the active fiber. The command codes are sent digitally by LED1 and are detected by PD2. Since the PD2 keeps listening to active fiber, the digit signals of "Start" command will be picked up by PD2. After the command is decoded, the control unit B makes the PD2 and PD4 ready for measurement signal detection and sends "Ready" command to active fiber by LED2. PD1 receives the "Ready"

command, and LED1 is turned on for a period of time ΔT as the light source for measurement. At this time, PD2 and PD4 can get continuous light signals but maybe not steady. The influence may come from the ambient temperature and transitional working state of LED. The control unit B evaluates the signal quality and makes the judgment. If the signal quality is not good, the control unit B will resend the "Ready" command and LED1 will be turned on again for repeated measurement. After the data from PD2 and PD4 are saved, the control unit B sends "Get ready" command to PD1. The control unit A makes PD1 and PD3 ready for measurement signal detection and then sends "Ready" to PD2. After the "Ready" command is received, LED2 is turned on for a time period of ΔT as the light source in opposite direction. Similar with the first step measurement, the control unit B evaluates the signal quality from PD1 and PD3 and makes the judgment whether to repeat the measurement or not. After the data from PD1 and PD3 are saved, control unit A sends "Data" command and the saved data of PD2 and PD4 in control unit B are transmitted to this side. Finally, all the data are processed by control unit A and it gives the final measurement results to I/O port of the sensor system.

Element	Fiber	Coupler	LED	Photodiode	Amplifier	μController with A/D
Number	2	2	2	2	4	2
Note	Multi-mode	3 dB	30μW	25fW NEP	High	46 dB Dynamic Range

Table 1. Basic Elements of Sensor System

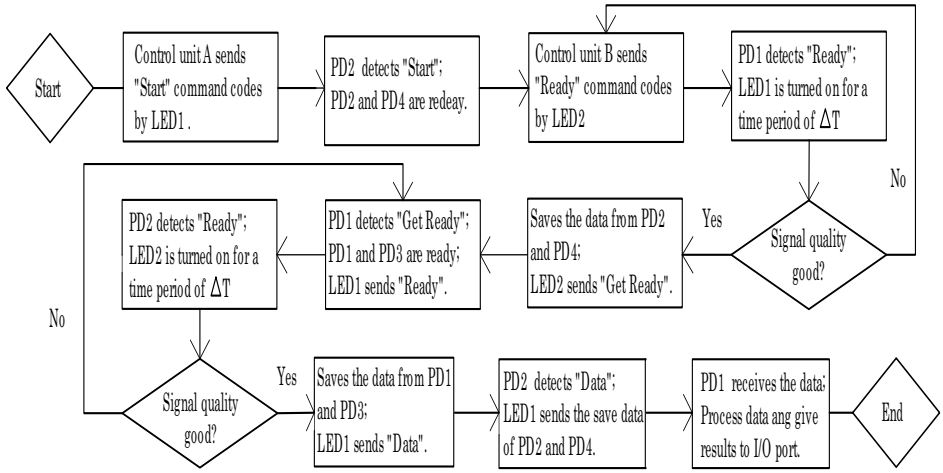

Fig. 11. Working flow chart of the sensor system

Using the active fiber as command communication medium, the sensor system can control the electric units in two physical positions without any additional signal channel. Since the control command is digital signal, the transmission rate change of active fiber caused by strain will not fail the communication as long as the light signal can be detected. Totally four

command can be coded by two bits data. The micro controller functions include control logic (two bits commands), control A/D, storing 4 numbers of data and communication for data upload to I/O. A simple micro controller can perform all the functions easily. It is noticeable that all the hardware in the sensor system from regular electrical and optical elements. There are no sophisticated circuits nor complex devices or special techniques used in the sensor system. The cost is dominated by the basic elements as listed in Table 1.

3.2 Theoretical Analysis on Limit Parameters

Double-ended light source gives symmetric coupling coefficient in the two direction of backward and forward. The output light power at the two ends of passive fiber can be expressed by equations (14) and (15) which is similar to but different with equations (4) and (5) in backward light power equation.

$$P_f = P_0 \cdot k_e \cdot 10^{-\frac{\alpha \cdot x}{10}} \cdot k_s \cdot 10^{-\frac{\beta(L-x)}{10}} \tag{14}$$

$$P_b = P_0 \cdot k_e \cdot 10^{-\frac{\alpha \cdot (L-x)}{10}} \cdot k_s \cdot 10^{-\frac{\beta \cdot x}{10}} \tag{15}$$

Since outputs of the passive fiber are used for position sensing, the length limiting conditions are that $P_f > P_{min}$ at position of x = 0 and $P_b > P_{min}$ at position of $x = L$. Here, P_{min} is the minimum detectable light power by photodiode preamp which is equal to n times of the noise equivalent power (NEP) and n is related to signal noise ratio. Because the symmetrical character of P_f and P_b, the two conditions are equivalent for theoretical length limit analysis. Educing equation (14) by this limiting condition, we can get the length limiting equation as follow:

$$L < \frac{10}{\beta} \log_{10}\left(\frac{P_0 \cdot k_e \cdot k_s}{NEP \cdot n}\right) \tag{16}$$

From equation (16), we get the theoretical length limit to passive fiber attenuation coefficient β, as shown in Fig. 12, where P_0 is equal to effective coupled light power of 30μW (LED L7560) and P_{min} values are 22 fW, 220 fW and 2.2 pW corresponding to R_F value of 10^{-9} Ω, 10^{-8} Ω and 10^{-7}Ω respectively. From the curves illustrated in Fig. 7, we know the sensor maximum length is dependent on the light coupling coefficient k_s, the passive fiber attenuation coefficient β and the P_{min} value of the light detection circuit. The k_s has been proved in the area of 10^{-5}~10^{-2}. By choosing appropriate attenuation coefficient for the passive fiber, the proposed sensor is possible to reach the level of kilometers. Given the conservative value of P_{min} = 2.2 pW, the maximum length is above kilometer when β is in the area of 10^{-3}~10^{-2} dB/m.

The spatial resolution of the proposed sensor is determined by the sensing element interval. As the precondition of effective sensing, the sensing element interval Δd must be greater than the minimum spatial resolution Δx which is determined by sensor design parameters. The minimum spatial resolution Δx by single end output is restricted by the conditions as expressed in equation (7) and (8).

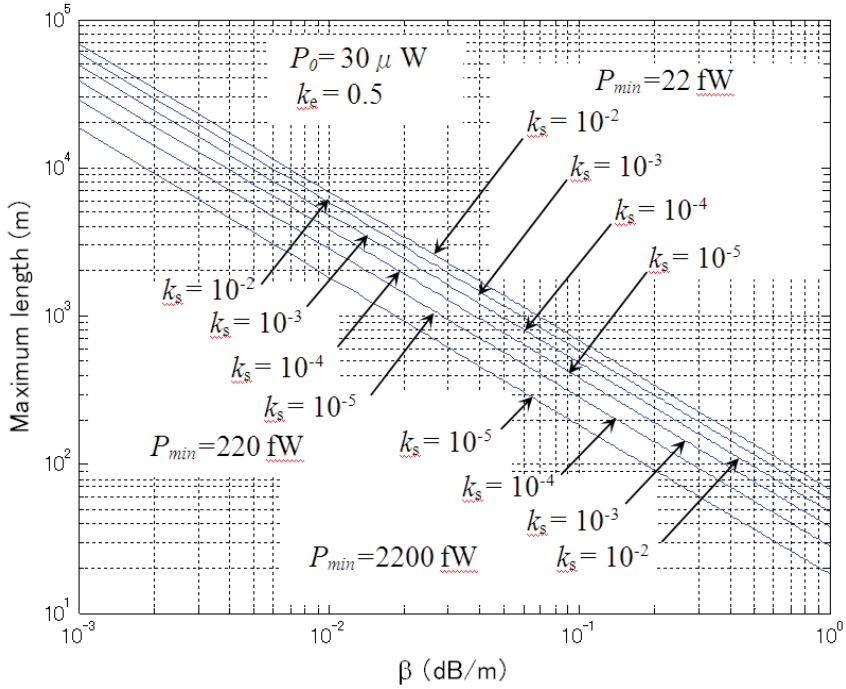

Fig. 12. Length limit of the sensor with different *NEP*

Similar with the analysis in Section 2.3, we can get the spatial resolution distribution along the fibers as shown in Fig. 13. Because of the exponential attenuation of light propagating in fiber, the spatial resolution of the proposed sensor is non-uniform along the fibers. Fig. 13 shows the single end determined spatial resolution along the fibers with given parameters of L=1000 m, α = 0.0002 dB/m, β = 0.001 dB/m. From Fig. 13, we know that the spatial resolution changes in large area from hundreds of meters to millimeter and is greatly dependent on the coupling coefficient and P_{min} value.

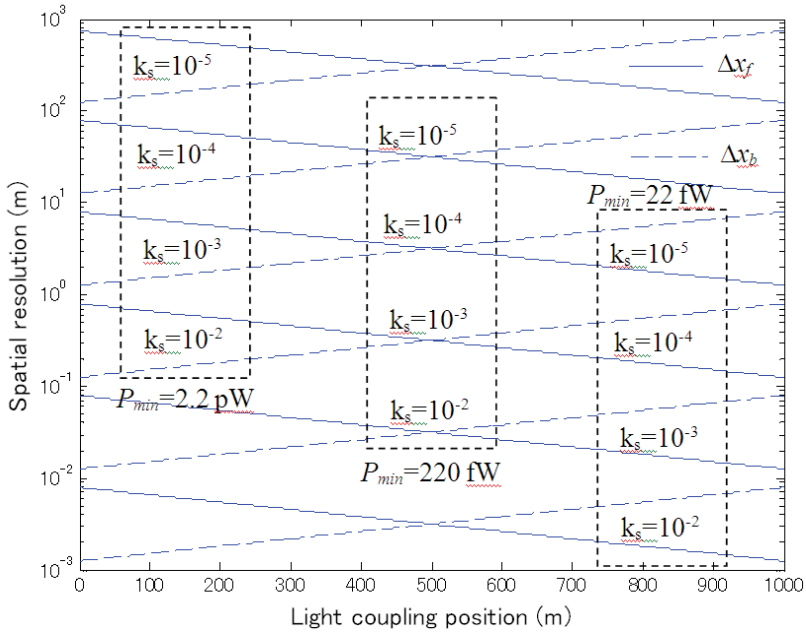

Fig. 13. Spatial resolution distribution along the fibers

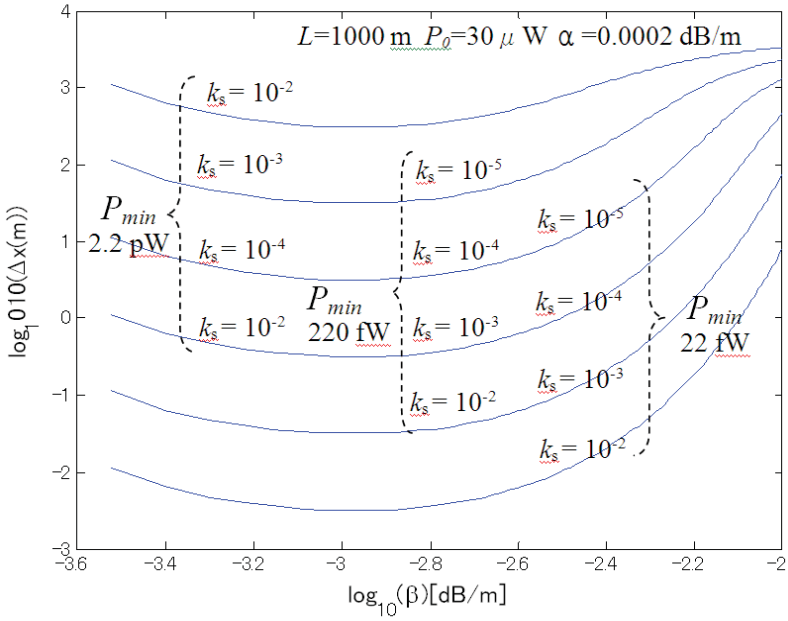

Fig. 14. Spatial resolution dependence on the attenuation coefficient β coupling coefficient k_s and *NEP*

Since the output light power at both ends of the passive fiber is dependent on the coupling coefficient k_s, we divide (14) by (15) and get position sensing function using double ended outputs as follow:

$$x = \frac{1}{2}[L + \frac{10}{\beta - \alpha}\log_{10}(\frac{P_f}{P_b})] \tag{17}$$

In equation (17), the strain position has no dependence on the coupling coefficient k_s in theory. Actually, position sensing by (17) is still influenced by k_s in sensitivity and SNR value. The sensing is also restricted by the limiting conditions for the length and spatial resolution. From Fig. 13, we know that the maximum values of Δx is at the position of $x = L/2$. Using this conservative condition, we show the double ended outputs determined spatial resolution with different parameters of β, k_s and P_{min} in Fig. 14.

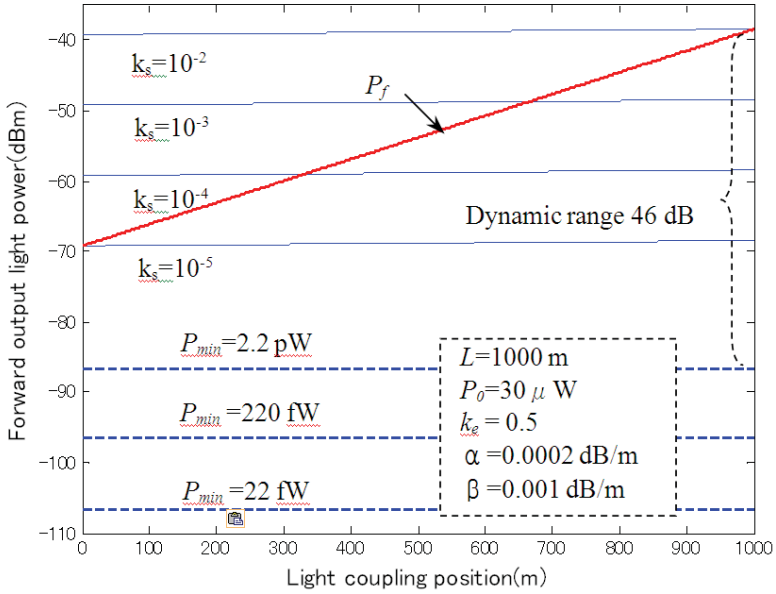

Fig. 15. Dynamic range of forward output light power of passive fiber

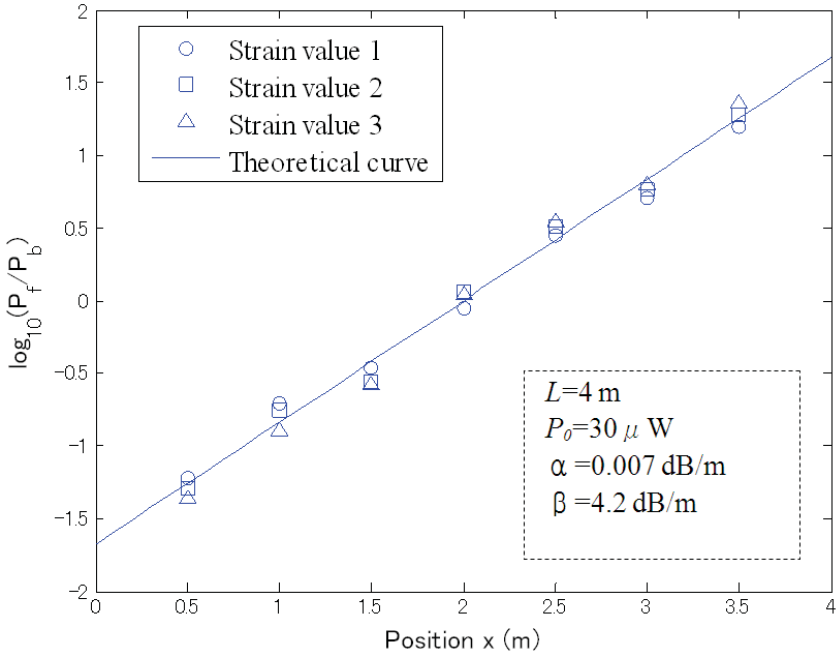

Fig. 16. Response of the passive fiber to distributed strain

The minimum spatial resolution are in the areas of (1 cm, 1 m) , (10 cm, 100 m) and (1 m, 1000 m) when the coupling coefficient value changes for 10^{-5} to 10^{-2} and P_{min} values are 22 fW, 220 fW and 2.2 pW respectively. As the limiting condition, sensing element interval should be greater than the minimum spatial resolution. According to specific needs, the sensing element interval can change in a large area from centimeters to hundreds meters.

The forward output light power of the passive fiber is shown in Fig. 15 with the given parameters values. The output light power is dependent on light coupling coefficient k_s and light attenuation in the two fibers. Under given conditions, the output light power has a dynamic range of 31 dB. The passive fiber attenuation coefficient value of 0.001 dB/m is chosen based on the length limit and spatial resolution analysis results for the length of 1000 m. The P_{min} lines of 2.2 pW, 220 fW and 22 fW are also shown in Fig. 15. From this figure, we can see that the passive fiber outputs have quite great safe space to the minimum detectable light power and the sensor can get quite great SNR value. A dynamic range of 46 dB (from -86 dBm to -38 dBm) is needed to be covered by the A/D converter for a minimum detectable light power of 2.2 pW. This can be realized using a 8-bit A/D converter (24 dB) and repetition increasing of 30 dB. Since the sensor use continuous signal form, there is no bandwidth requirement for both of light source and light detector. Within a bandwidth of 1 Hz, the signal can be detected by simple photodiode preamp circuit which can have a great dynamic range. All the performance parameters of the sensor are specially designed for specific applications requirements. For other circumstances, the sensor parameters values should be redesigned taking the specific applications considered.

3.3 Experiments and Results

In order to confirming the sensor, a prototype sensor is developed in the length of 4 m in laboratory. In Fig. 16, we show the experimental results in strain position sensing with the corresponding theoretical curves. Totally seven sensing elements are used which have uniform interval of 0.5 m. The parameters used in prototype sensor are as follows: α = 0.007 dB/m, β = 4.2 dB/m, P_{min}= 2.2 mW (R_F =10^4 Ω). Three stain values are applied in the experiments which lead to different coupling coefficient value of k_s. From Fig. 16, we can see that, the position sensor results have no dependence on the strain value and the experimental results are well coincident to the curves predicted by theoretical equation (17). Using the double ended light source and sensing element, the sensor gets symmetrical outputs at the two ends of the passive fiber. It contributes the promotion of sensor performance parameters including length, spatial resolution and appropriate dynamic range and makes the proposed sensor possible for practical applications.

4. Discussions and Conclusions

4.1 Discussions

The multi-fiber model sensor has lower cost and simpler principle compared with other distributed optical sensor. The advantages of multi-fiber model sensor are discussed as following:

(1) There is no special structure in the fibers like bragg grating. There are also no special requirements for the optical fiber such as light wavelength, homochromy, interference, polarization and dispersion. A wide range of optical fiber can be the candidates in designing and fabricating sensors.

(2) The sensor has no critical requirements on light source and signal detection instruments. The sensor has light intensity based outputs for both of the active fiber and the passive fiber. By using continuous form signals, the sensor needs no great bandwidth for both of the light source and the light detector circuit. This is greatly helpful to improve the signal to noise ratio and sensor sensitivity and reduce the complexity and cost of signal detection hardware.

(3) The driving and control circuits are simple and low cost. Totally, four commands are used in handshake process which can be encoded by two bits. The digital pulses for handshake need neither critical up and down edges nor great bandwidth. The data saving and processing require only four numbers' memory space and simple calculation ability which can easily realized by a single chip.

Therefore, the sensor has the simple and low cost characters which will contribute to wider application of the optical fiber sensors. It is a competitive solution to distributed parameters measurement in medium length distance (several meters to kilometers).

The main limitation of the proposed sensor is the difficulty for multipoint measurement at the same time. But there are many circumstances where the first problem point is of the most interests, for example, the safety monitoring of civil structure. It is meaningful in many applications to alert and locate the first problem point. After appropriate modification, the sensor is possible to be used in submersion sensor, hot spot sensor, inner deformation sensor, position sensor and so on. The multi-fiber sensor makes the optical fiber sensor possible to be applied in wider circumstances where the conventional sensors may be not cost-effective. And it also makes complete the applications of distributed

optical fiber sensors in medium distance (several meters to 1 kilometer) as a low cost solution.

4.2 Conclusions

In this chapter, we introduced a novel quasi-distributed optical fiber for distributed strain monitoring. By using the coupling light between two multi-model fibers, the sensor gets output light intensity signals which can effectively be detected by photodiodes with common preamp circuit. The effectiveness of the sensor is practically confirmed. Theoretical analysis shows that the sensor's maximum length can reach the level of kilometers and the spatial resolution can reach the level of centimeters. In the distributed optical fiber sensor field, the proposed double-fiber model sensor is new attempt different from other techniques. Since the sensor uses neither sophisticated instruments nor any special techniques, the total systems can be realized with extremely low cost. It is meaningful to the widely needed on-line monitoring applications in many circumstances especially where the cost-effectiveness is critical limited.

5. References

A. J. Rogers, "Polarization optical time domain reflectometry," *Electron. Lett.*, vol. 16, pp. 489-490, Jun. 1980.

B. Lee, "Review of the present status of optical fiber sensors," *Opt. Fiber Technol*, vol. 9, pp. 57-79, Apr. 2003.

C. Wang and K. Shida, A novel multifunctional distributed optical fiber sensor based on attenuation, *Proc. IMTC'06*, pp. 2018-2023, April, 2006.

C. Wang and K. Shida, A low cost double-fiber model distributed optical fiber sensor, *IEEE T. Instrum. Meas.*, Vol. 56, No. 4, August, 2007.

C. Wang, Study on Multifunctional Sensors for Trucks Safety Monitoring, Ph.D Thesis of Saga University, September, 2007.

J. P. Dakin, D.J. Pratt, G.W. Bibby, J. N. Ross, "Distributed optical fiber Raman temperature sensor using a semiconductor light source and detector," *Electron. Lett.*, vol. 21, pp. 569-570, Jun. 1985.

J. K. A. Everard, Novel signal techniques for enhanced OTDR sensors, *Proc. SPIE*, vol. 798, pp. 42-46, Mar. 1987.

L. Thevenaz, M. Facchini, Monitoring of large structures using distributed Brillouin fiber sensing, *Proc. OFS'13*, pp. 345-348, 1999.

M. K. Barnoski and S. M. Jensen, Fiber vaveguides: A novel technique for investigating attenuation characteristics, *Appl. Opt.*, vol. 15, pp. 2112-2115, 1976.

M. Nakazawa, Rayleigh backscattering theory for single-mode optical fibers, *Opt. Soc. Am.*, vol. 73, no. 9, pp. 1175-1180, Sep. 1983.

M. Zaboli, P. Bassi, High spatial resolution OTDR attenuation measurement by a correlation technique, *Appl. Opt.*, vol. 22, pp. 3680-3681, Dec. 1983.

M. Tateda, First measurement of strain distribution along field installed optical fibers using Brillouin spectroscopy, *J. Lightwave Technol.*, vol. 8, pp. 1269-1272, 1990.

W. Eickhoff and R. Ulrich, Optical frequency domain reflectometry in single-mode fiber, *Apply. Phys. Lett.*, vol. 39, pp.693-695, Nov. 1981.

W. W. Morey, G. Meltz, and W. H. Glenn, Fiber Bragg grating sensors, *Proc. SPIE*, vol. 1169, pp. 98-107, Jan. 1990.

W. L. Schulz, E. Udd, J. M. Seim, and G. E. McGill, Advanced fibre grating strain sensor systems for bridges, structures, and highways, *Proc. SPIE*, vol. 3325, pp. 212-221, 1998.

Optical Fiber New Developments

Edited by Christophe Lethien

ISBN 978-953-7619-50-3
Hard cover, 586 pages
Publisher InTech
Published online 01, December, 2009
Published in print edition December, 2009

The optical fibre technology is one of the hop topics developed in the beginning of the 21th century and could substantially benefit applications dealing with lighting, sensing and communication systems. Many improvements have been made in the past years to reduce the fibre attenuation and to improve the fibre performance. Nowadays, new applications have been developed over the scientific community and this book fits this paradigm. It summarizes the current status of know-how in optical fibre applications and represents a further source of information dealing with two main topics: the development of fibre optics sensors, and the application of optical fibre for telecommunication systems.

INTECH
open science | open minds

InTech Europe
University Campus STeP Ri
Slavka Krautzeka 83/A
51000 Rijeka, Croatia
Phone: +385 (51) 770 447
Fax: +385 (51) 686 166
www.intechopen.com

InTech China
Unit 405, Office Block, Hotel Equatorial Shanghai
No.65, Yan An Road (West), Shanghai, 200040, China
中国上海市延安西路65号上海国际贵都大饭店办公楼405单元
Phone: +86-21-62489820
Fax: +86-21-62489821